Hydrazine Doped Graphene and Its Stability

MinHo Song[a], Somyeong Shin[a], Taekwang Kim[a], Hyewon Du[a], Hyungjun Koo[a],

Nayoung Kim[b], Eunkyu Lee[b], Seungmin Cho[b], and Sunae Seo[a,*]

[a]*Department of Physics, Sejong University, Seoul 143-747*
[b]*Micro Device&Machinery Solution Division, Samsung Techwin R&D Center, Seongnam 463-400*

The electronic property of graphene was investigated by hydrazine treatment. Hydrazine (N_2H_4) highly increases electron concentrations and up-shifts Fermi level of graphene based on significant shift of Dirac point to the negative gate voltage. We have observed contact resistance and channel length dependent mobility of graphene in the back-gated device after hydrazine monohydrate treatment and continuously monitored electrical characteristics under Nitrogen or air exposure. The contact resistance increases with hydrazine-treated and subsequent Nitrogen-exposed devices and reduces down in successive Air-exposed device to the similar level of pristine one. The channel conductance curve as a function of gate voltage in hole conduction regime keeps analogous value and shape even after Nitrogen/Air exposure specially whereas, in electron conduction regime change rate of conductance along with the level of conductance with gate voltage are decreased. Hydrazine could be utilized as the highly effective donor without degradation of mobility but the stability issue to be solved for future application.

I. Introduction

Graphene doping, which could tune charge carrier concentration along with carrier type, becomes main research topic for applications such as transparent electrode or semiconducting channel node of tran–sistor [1]. The chemical doping has been generally executed by covalent or noncovalent functionalization of molecular materials [2]. The electronic properties of graphene can also be tuned by the chemical mod–ification such as partial or full hydrogenation [3] and fluorination [4]. However the strong covalent bond such as C–H and C–F disturbs sp2 hybridization of carbon atoms and induces structural defects or chemical impurities, which could highly affect the electronic band structure and transport property of graphene. On the other hand, the doping by the sur–face charge transfer due to the electron exchange at the interface of graphene and dopants leaves the electronic structure of graphene intact [5]. This is usually achieved by molecular materials absorbed on the surface of graphene. Molecules with electron

withdrawing or donating groups will lead to p-type or n-type doping to graphene by charge transfer, respectively [5]. Accordingly, graphene can be intentionally doped by depositing organic or inorganic materials such as alkali metal atoms or aromatic molecules on its surface [6].

There still exist two main issues regarding graphene doping utilized by charge transfer. First, despite of undisturbed electronic structure of graphene by charge transfer doping, the mobility of graphene has been reported to be degraded by the dopant that could play a role of charged impurity center since it is dominated not by the lattice vibration but the charged impurities at the room temperature [7]. Second, it is significantly difficult to accomplish required stability for device application.

Among the various dopants, highly effective work function changes are obtained using acid or base materials. Hydrazine (N_2H_4), strong base, was introduced to reduce graphene oxide into graphene [8]. More recently, diluted hydrazine monohydrate solution was adapted as the n-type dopants using its unpaired electron [9]. Here, we monitor graphene Fermi level shift using highly diluted N_2H_4 solution and investigate the stability issue along with trans-

port property. N_2H_4 treatment is very effective to dope graphene with negligible mobility degradation but requires the reliable doping stability as expected.

II. Experimental Results

Chemical vapor deposition (CVD) graphene on Cu foil was transferred onto SiO_2/Si wafer using polymethyl methacrylate (PMMA) and patterned by photolithography [10]. Device structure is shown Fig. 2. Source and Drain electrodes are formed using thermal evaporation of Au and succeeding lift-off process with 10 um distance on the graphene bar. Channel width of graphene transistor is 200 μm. After device fabrication, graphene is annealed under vacuum at 250°C for 6 hours to remove PMMA residue, which can generate unintentional hole doping of graphene [10]. Then, device is soaked for 10 second in Hydrazine Monohydrate solution diluted by de-ionized water (1:9) for N_2H_4 treatment. We took x-ray photoemission of N1s edge and C1s edge and obtained small N1s edge signal with only N_2H_4 treated devices. Also, C1s showed broadened signal at high binding energy. (Data is not included) Raman spectroscopy is taken using laser of 514 nm wavelength after device fabrication. The channel conductance is measured by 4-point probe method. The device parameters such as mobility or Dirac point are investigated.

Raman data normalized by G peak intensity (I_G) were taken to monitor graphene during the device fabrication process, which is shown in Fig. 1. Although the slight increase of the normalized D peak intensity (I_D/I_G) is found in graphene after vacuum annealing, it appears nearly negligible. I_{2D}/I_G ratio is elevated from 1.5 to 2.5 during the graphene transfer, photolithography and vacuum anneal. The initial low I_{2D}/I_G value could be originated from hole-doping of graphene judging by the shift of G peak whose positions after transfer, photolithography and vacuum
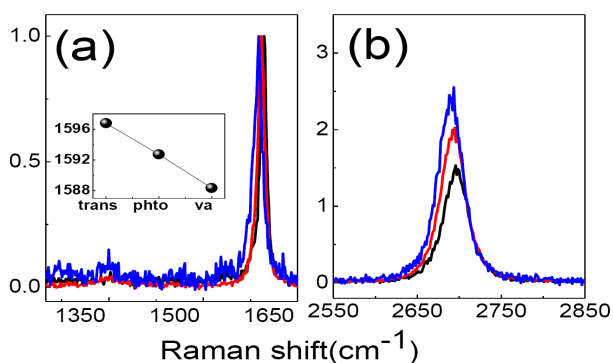

Figure 1. Raman data normalized by I(G) peak. (a) G peak, (b) 2D peak. Inset: G peak shift with process. Black: after graphene transfer (trans), Red: photolithography for device fabrication (photo) Blue:vacuum annealing (va).
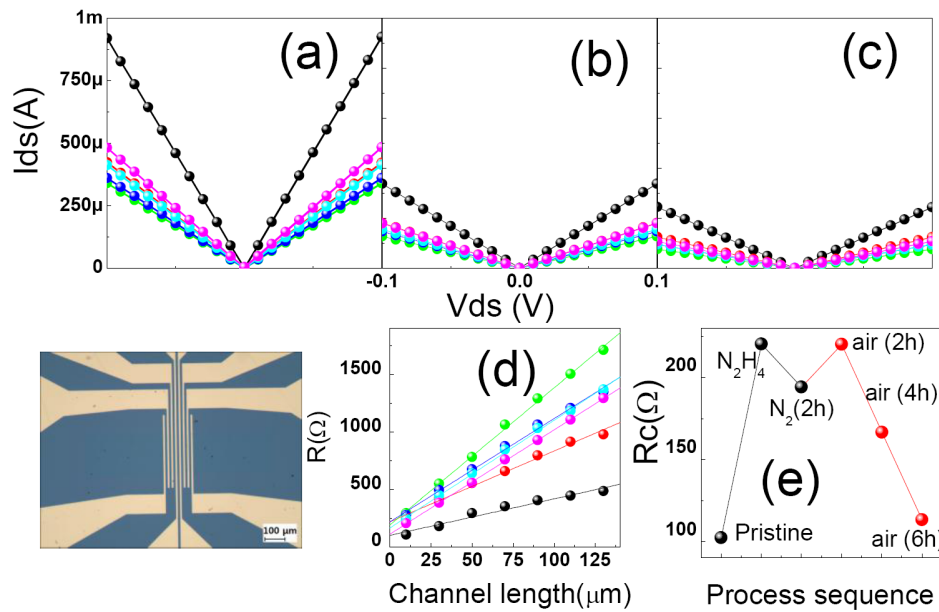
MinHo Song, Somyeong Shin, Taekwang Kim, Hyewon Du, Hyungjun Koo, Nayoung Kim, Eunkyu Lee, Seungmin Cho, and Sunae Seo

Figure 2. Channel current as a function of Source/ Drain voltage (I_{ds}−V_{ds}) (a) 10, (b) 50, (c) 90 μm. (d) channel length dependent resistance. (e) Contact resistance extracted from (d). In (a–d), Black: pristine, Red: N_2H_4 doping, Green: 2 hour N_2 exposure, Blue: 2 hour, Cyan: 4 hour, Purple: 6 hour under ambient. Inserted picture: Fabricated device structure.

annealing are 1,596, 1,592 and 1,587 cm^{-1} respectively. According to the density functional theory (DFT) calculation, G peak stiffening from 1,584 cm^{-1} and I_{2D}/I_G ratio decrease around 3 in intrinsic graphene are significant with the increase of charge carrier concentration [11]. Therefore, G peak softening along with 2D intensity boost indicate that the raised charge carrier concentration during the transfer is lowered by following processes such as device fabrication and vacuum anneal. Hole−doping by PMMA residue used as the sacrificial layer during graphene transfer is known to be responsible for the carrier density increase [12]. Vacuum annealing about 200∼250°C helps removing these adsorbed residues.

In order to study electrical property of N_2H_4−treated graphene device, channel current (I_{ds}) with applied Source/Drain voltage (V_{ds}) at gate floating is measured with the device of 10, 50 and 90 μm channel length as shown in the Fig. 2(a), (b) and (c). I_{ds} versus V_{ds} (I_{ds}−V_{ds}) shows metallic behavior in all the measured devices before and after N_2H_4 treatment. Total resist−

ance is plotted in Fig.2(d) from the slope of I_{ds}−V_{ds} curve. We have obtained contact resistances of all the devices from y−axis interception in curves of Fig. 2(d) using following equation. $R_{tot}=R_c+R_s(L/W)=V_{ds}/I_{ds}$, where R_{tot}, R_c and R_s mean total resistance, contact resistance and channel sheet resistance respectively. L and W indicate channel length and width of measured device.

Fig. 2(e) represents the extracted contact resistance. N_2H_4 treatment doubles the contact resistance of pristine device. The change of contact resistance is unexpected since we soaked graphene in N_2H_4 solution after the completion of device. It is probably due to the diffusion of N_2H_4 into the interface of graphene and Au electrode. The charge carrier injection from electrode to graphene could be hindered by diffused N_2H_4. After 6 hour exposure, it is recovered to the similar level of pristine device.

The electrical transport in graphene transistor is measured by 4 point probe technique using current source. The channel resistance curves of different

194

Appl. Sci. Conv. Technol. 23(4), 192-199 (2014)

channel length of 10, 50 and 90 um are represented in Fig. 3(a),(b) and (c). Neutral point (V_{NP}), the gate voltage of maximum channel resistance, is located between 60~70 V in pristine device (first measurement) and is displaced below -80 V after N_2H_4 treatment (second measurement), that indicates electron doping by hydrazine treatment. After electrical property measurement, we had preserved all the N_2H_4-treated devices for 2 hours in Nitrogen filled glove box and then re-measured the channel resistance(third measurement), which is green line data of Fig. 3(a),(b) and (c). V_{NP} of those curves already shifts to the gate voltage of -40~-35 V range by N_2 exposure. After third measurement, we left devices exposed to the ambient for hours and measured channel resistance after 2, 4 and 6 hours exposure. V_{NP} continues to shift to the positive side. Unlike N_2 exposure, the maximum resistance at V_{NP} decreases by Air exposure.

From channel resistance curves, we re-plotted the channel conductance data by moving neutral point to origin, which are shown in Fig. 3(d), (e) and (f). The conductance curves of different channel length seem to show common behavior regardless of channel length. The conductance evolution with N_2 or Air exposure looks more stationary in hole-conduction regime than in electron-conduction regime. Hole conduction behavior remains affected during the N_2 or Air exposure without noticeable change. On the other hand, conductance is highest after N_2H_4 treatment in electron conduction regime. Unfortunately, we could not obtain the electron conduction in pristine and hole conduction in N_2H_4-treated devices due to extreme hole and electron doping and thus could not explain the influence on conductance by hydrazine treatment except for the gate voltage close to V_{NP}. N_2H_4 treatment enhance the conductance close to minimum conductivity point judging by the curve shape close to V_{NP} as shown in the inset of Fig. 3(d), (e) and (f). [13]

Fig. 4 (a) shows the minimum conductivity (σ_{min}) change depending on the process at the V_{NP} (Fig. 4(b)). σ_{min} is closely related to the residual impurity and re-
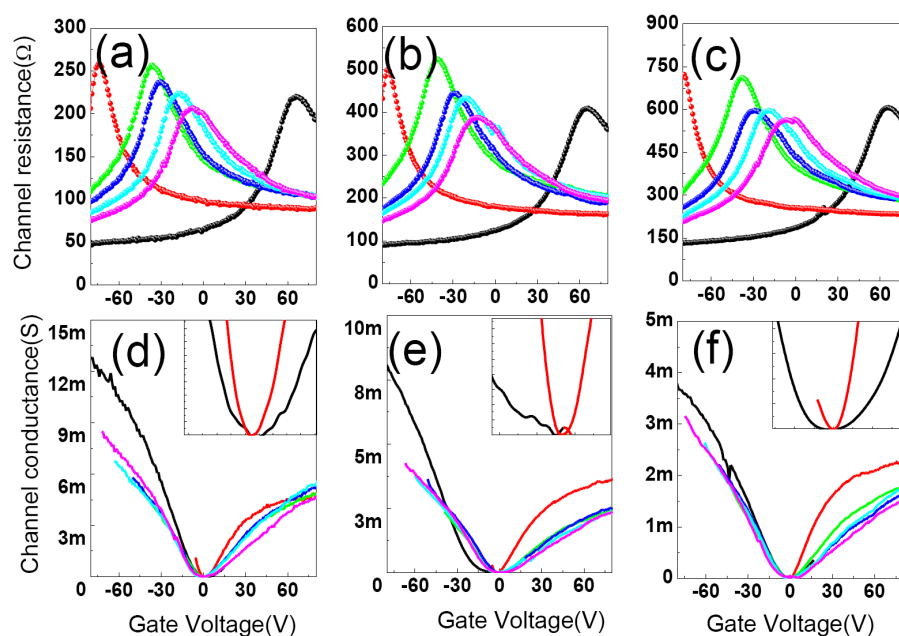

Figure 3. Gate voltage dependent channel resistance with different channel length after N_2H_4 doping (a) 10, (b) 50, (c) 90 μm. Gate voltage dependent channel conductance after moving V_{NP} into the origin (d) 10, (e) 50, (f) 90 μm. In (a–f), Black; pristine, Red; N_2H_4 doping, Green; 2 hour N_2 exposure, Blue; 2 hour, Cyan; 4 hour, Purple; 6 hour under ambient. Inset of (d–f) : expanded V_{NP} area.
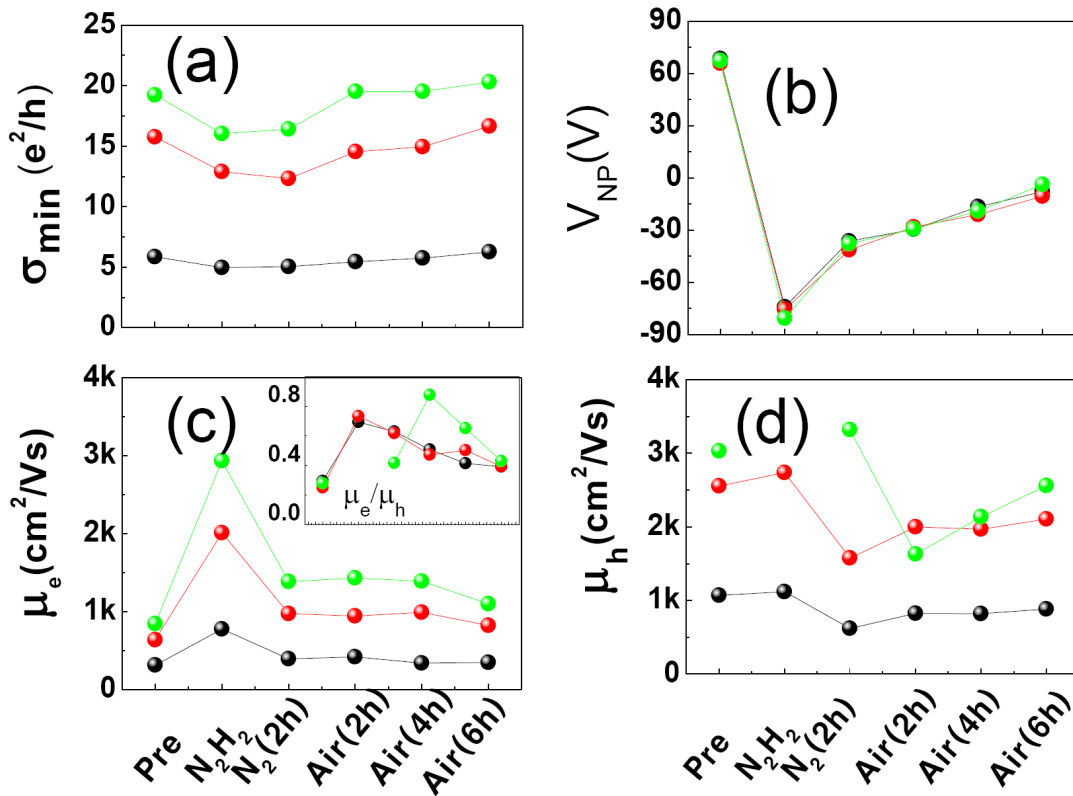
MinHo Song, Somyeong Shin, Taekwang Kim, Hyewon Du, Hyungjun Koo, Nayoung Kim, Eunkyu Lee, Seungmin Cho, and Sunae Seo

Figure 4. (a) Minimum conductivity (σ_{min}), (b) V_{NP}, (c) Electron mobility (d) Hole mobility. In (a–d), Black : 10, Red: 50, Green: 90 μm. Inset of (c): the ratio of electron to hole mobility.

versely proportional to the carrier mobility which is generally dominated by charged defects in graphene [6,13]. Therefore, process dependent σ_{min} V_{NP} can illustrate the variation of dopant concentration and inhomogeneous residual charge distribution at the low carrier density. N_2H_4 treatment shifts V_{NP} to highly negative voltage side while it lowers σ_{min} and increases mobility. But subsequent N_2 exposure reshapes V_{NP} and mobility to return to the pristine state with keeping similar σ_{min}. Then, next exposure under ambient condition recovers σ_{min} and mobility to pristine state and V_{NP} to the intrinsic Dirac Point.

Also, lowest σ_{min} and mobility are obtained at 10 nm channel length device as shown Fig. 4(a), (c) and (d). The conductance close to neutral point is caused by residual impurity or electron–hole puddle. Therefore, low σ_{min} is expected to show high mobility as previously mentioned. However, in our devices, op-

posite effects were observed. This phenomenon might be also related with the channel length dependent mobility increase as shown in Fig. 4(c) and (d), which is improbable in diffusive conduction regime. It's unclear but one of reasons could be in invasive Source/Drain electrode structure we have utilized. The metal electrode on graphene can change work function of graphene and also carrier density. In addition, the electronic band structure change of graphene could be caused by the stress due to upper metal electrode. If we deal with long channel, we have wider region of metal/graphene stack structure in our device structure. Since we soak graphene device with pre-deposited Source/Drain metal electrode during N_2H_2 treatment, there exists area we cannot control and attach dopants on graphene. Those combined effects by overlapped metal electrodes could be responsible for the unusual behavior of conductivity

196

Appl. Sci. Conv. Technol. **23**(4), 192-199 (2014)

and mobility.

Highly increased electron mobility with hydrazine treatment becomes reduced by N_2 or Air exposure. Whereas, although hole mobility of N_2H_4 treated device is difficult to measure due to the large V_{NP} shift due to hydrazine treatment, hole mobility does not change with N_2H_2 treatment based on the slope of gate dependent channel conductance curve close to V_{NP} as shown in the inset of Fig. 3(d−f) It is rather reduced by N_2 exposure and then gradually recovered with Air exposure. For the CVD graphene, hole mobility often has been reported to be higher than electron one [14]. Electron and hole conduction asymmetry has been considered by various mechanisms [15−18]. Here, the electron to hole mobility ratio shown in the inset of Fig. 4 indicates the asymmetry is induced by doping [15]. P−type (n−type) doping produces a potential barrier that suppresses electron (hole) conductance and preserves hole (electron) conductance except for initial hydrazine treatment. It was explained that homogeneous potentials created by long range scatters cause conductance suppression of only one carrier type.

Our previous conductance curves are ones obtained from forward gate voltage sweep of −80 V to 80 V. We have attempted to observe hysteresis of forward and reverse voltage sweep for the channel current. The conductance hysteresis on the device of 50um channel length is plotted in Fig. 5. V_{NP} values of all the curves are higher in reverse sweep direction than in forward sweep. This gap in both sweep direction is smallest in the pristine device and largest in hydrazine treated devices. Specially, R−Vg in the direction of reverse sweep on the hydrazine treated device looks very flattened at hole conduction regime, which exhibits highly asymmetric conductance curve generated by the suppression of hole conduction. With N_2 or Air exposure, conduction curve becomes more symmetric with sweep direction and the gap of V_{NP} is lessened.

The electronegative or electropositive material doping of graphene are expected to lead to a decrease
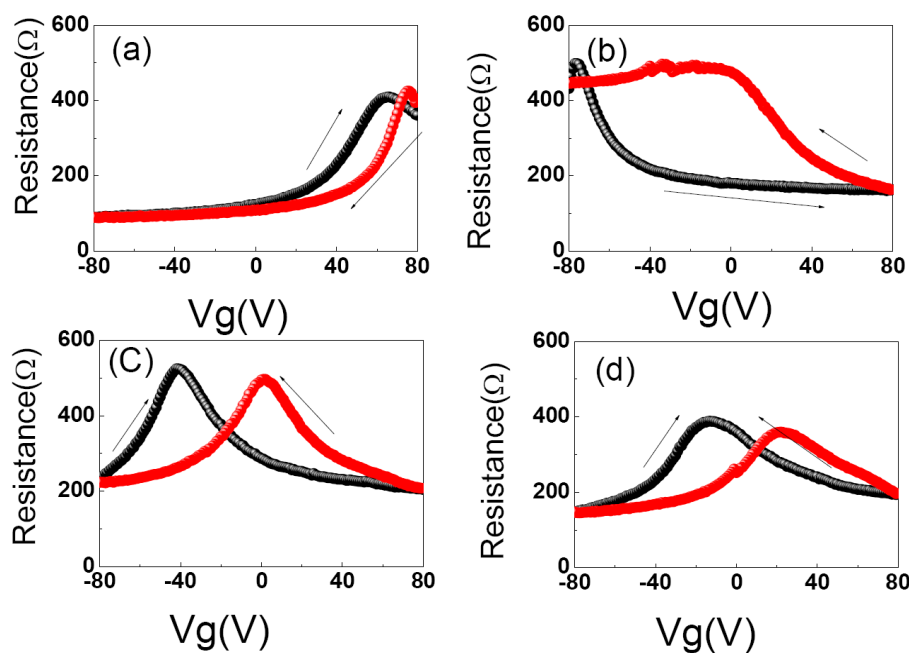

Figure 5. Hysteresis of channel conductance on graphene device with the direction of forward and reverse gate voltage sweep. (a) Pristine, (b) N_2H_4 treatment, (c) 2 hour N_2 exposure, (d) 6 hour ambient exposure.
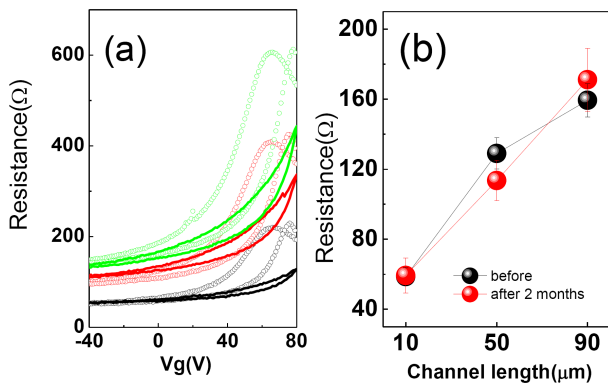
MinHo Song, Somyeong Shin, Taekwang Kim, Hyewon Du, Hyungjun Koo, Nayoung Kim, Eunkyu Lee, Seungmin Cho, and Sunae Seo

Figure 6. Gate voltage dependent channel current (a) open symbol; prestine, line; 2 months exposure to Air after N_2H_4 treatment. Black; 10 μm, Red; 50 μm, Green; 90 μm (b) channel resistance measured at zero gate voltage.

in carrier mobility arising from Coulomb scattering but without any hysteresis whereas electrochemical doping is effected by redox reactions and shows large hysteresis [19]. This hysteresis could be explained by dipolar adsorbates such as water. The hysteresis is suppressed or vanishes when placing graphene in vacuum and pumping for an extended time. In our devices, loosely bound species are the main culprits for hysteresis [20]. The rapid V_{NP} change and hysteresis reduction after exposure to N_2 or Air within several hours might be originated from the weak interaction between adsorbates and graphene.

In other to investigate the stability of hydrazine treated graphene device, gate dependent channel resistance has been measured after exposure for two months. The higher hole doping is observed compared with pristine graphene device judging by V_{NP} shift larger than 80 V (applied maximum positive voltage. It seems that a highly effective electron doping on graphene produced by hydrazine treatment could not be retained under the atmospheric environment. It might be caused by weak binding of graphene and dopant or chemical interaction between dopant and H_2O or O_2 gas, which could explain more increased hole doping after hydrazine doping. For the quantitative comparison, channel resistance at zero gate

voltage was replotted in Fig. 6(b). No distinctive difference was not detected with channel length.

One interesting point is that channel resistance was measured using four probe method. Therefore, it does not include the contribution of contact resistance. From the Fig. 6(b), we extracted the y-axis intercept using line fitting in both devices, which must be zero without contact resistance. They are 44, 52 Ohm for pristine and 2 month Air-exposed device after hydrazine treatment respectively. This channel length independent value could be related to the invasive electrode structure and abnormal relationship between minimum conductivity and mobility.

III. Summary

N_2H_4 could play a role of higly prouctive electron donor for graphene. It does not induce severe degradation of mobility but too unstable to adopt N_2H_4 treatment without considering passivation. In the initial stage of N_2H_4 treatment, mobility change of electron and hole appears dominated by long range scatters and the contact resistance between graphene and Source/Drain elctrode increases. But with exposure under N_2 or air, several device parameters such as mobility, channel conductance and contact resistance recover to the level of undoped states by relaxation. In addition V_{NP} exhibts the higher hole doping compared with the pristine graphene device without having hydrazine treatment. For N_2H_4 doping, to utilize this method to the real device application, primary issue to settle is how to control and acquire the device stability.

Acknowledgement

198

Appl. Sci. Conv. Technol. **23**(4), 192-199 (2014)

References

[1] S. De and J. N. Coleman, ACS Nano **4**, 2713-2720 (2010).

[2] V. Georgakilas, M. Otyepka, A. B. Bourlinos, V. Chandra, N. Kim, K. C. Kemp, P. Hobza, R. Zboril and K. S. Kim, Chemical Reviews **112**, 6156-6214 (2012).

[3] D. C. Elias, R. R. Nair, T. M. G. Mohiuddin, S. V. Morozov, P. Blake, M. P. Halsall, A. C. Ferrari, D. W. Boukhvalov, M. I. Katsnelson, A. K. Geim and K. S. Novoselov, Science **323**, 610-613 (2009).

[4] D. W. Boukhvalov and M. I. Katsnelson, Journal of Physics: Condensed Matter **21**, 344205 (2009).

[5] H. Liu, Y. Liu and D. Zhu, Journal of Materials Chemistry **21**, 3335-3345 (2011).

[6] J. H. Chen, C. Jang, S. Adam, M. S. Fuhrer, E. D. Williams and M. Ishigami, Nat Phys **4**, 377-381 (2008).

[7] S. Adam, E. H. Hwang, V. M. Galitski and S. Das Sarma, Proceedings of the National Academy of Sciences **104**, 18392-18397 (2007).

[8] S. Park, Y. Hu, J. O. Hwang, E.-S. Lee, L. B. Casabianca, W. Cai, J. R. Potts, H.-W. Ha, S. Chen, J. Oh, S. O. Kim, Y.-H. Kim, Y. Ishii and R. S. Ruoff, Nat Commun **3**, 638 (2012).

[9] I.-Y. Lee, H.-Y. Park, J.-H. Park, J. Lee, W.-S. Jung, H.-Y. Yu, S.-W. Kim, G.-H. Kim and J.-H. Park, Organic Electronics **14**, 1586-1590 (2013).

[10] Y.-C. Lin, C.-C. Lu, C.-H. Yeh, C. Jin, K. Suenaga and P.-W. Chiu, Nano Letters **12**, 414-419 (2011).

[11] DasA, PisanaS, ChakrabortyB, PiscanecS, S. K. Saha, U. V. Waghmare, K. S. Novoselov, H. R. Krishnamurthy, A. K. Geim, A. C. Ferrari and A. K. Sood, Nat Nano **3**, 210-215 (2008).

[12] J. Kang, D. Shin, S. Bae and B. H. Hong, Nanoscale **4**, 5527-5537 (2012).

[13] Y. W. Tan, Y. Zhang, K. Bolotin, Y. Zhao, S. Adam, E. H. Hwang, S. Das Sarma, H. L. Stormer and P. Kim, Physical Review Letters **99**, 246803 (2007).

[14] Y. Lee, S. Bae, H. Jang, S. Jang, S.-E. Zhu, S. H. Sim, Y. I. Song, B. H. Hong and J.-H. Ahn, Nano Letters **10**, 490-493 (2010).

[15] D. B. Farmer, R. Golizadeh-Mojarad, V. Perebeinos, Y.-M. Lin, G. S. Tulevski, J. C. Tsang and P. Avouris, Nano Letters **9**, 388-392 (2008).

[16] W. R. Hannes, M. Jonson and M. Titov, Physical Review B **84**, 045414 (2011).

[17] B. Huard, N. Stander, J. A. Sulpizio and D. Goldhaber-Gordon, Physical Review B **78**, 121402 (2008).

[18] R. Nouchi, M. Shiraishi and Y. Suzuki, Applied Physics Letters **93**, 152104 (2008).

[19] H. Pinto, R. Jones, J. P. Goss and P. R. Briddon, physica status solidi (a) **207**, 2131-2136 (2010).

[20] M. Lafkioti, B. Krauss, T. Lohmann, U. Zschieschang, H. Klauk, K. v. Klitzing and J. H. Smet, Nano Letters **10**, 1149-1153 (2010).